A new approach to analyse effects of nanoparticles on lipid vesicles

Jernej Zupanc

Faculty of Computer and Information Science,
University of Ljubljana, SI-1000 Ljubljana, Slovenia
E-mail: jernej.zupanc@fri.uni-lj.si

Janez Valant and Damjana Drobne*

Biotechnical Faculty, Department of Biology,
University of Ljubljana, SI-1000 Ljubljana, Slovenia
E-mail: janez.valant@bf.uni-lj.si
E-mail: damjana.drobne@bf.uni-lj.si
*Corresponding author

Veronika Kralj Iglič

Faculty Medicine, Laboratory of Clininical Biophysics,
Univ Ljubljana, SI-1000 Ljubljana, Slovenia
E-mail: veronika.iglic@fe.uni-lj.si

Aleš Iglič

Physics Laboratory, Faculty of Electrical Engineering,
Univ Ljubljana, SI-1000 Ljubljana, Slovenia
E-mail: ales.iglic@fe.uni-lj.si

Abstract: Manufactured nanoparticles are potentially capable of inducing defects in lipid membranes. The effects of nanoparticles on cell membranes are one of the key issues in nanomedicine, nanotoxicology, food and pharmaceutical application of products of nanomaterials and others. Our aim is to demonstrate the nanoparticle – lipid vesicle interactions and to develop a controllable experimental setup for data acquisition. We studied interactions between nanoparticles (C_{60}) and lipid vesicles (POPC), using $ZnCl_2$ as a positive control. Light microscopy computer aided image segmentation was developed and population differences among vesicles incubated in different media were assessed. Data obtained by statistical image analysis methods revealed that nanoparticles (C_{60}) caused changes in vesicle size distribution in the population of lipid vesicles as well as a burst of vesicles in time and in a concentration gradient. No significant changes in shape of vesicles were recorded. The advantage of the experimental set up presented here is that it employs statistical image analysis methods and direct microscopy observation of large populations of lipid vesicles. We discuss the applicability of this *in vitro* approach in analysing the effects of nanoparticles on simplified biological membranes.

Keywords: lipid vesicles; POPC; nanotoxicity; nanoparticles; C_{60}; computational microscopy.

Copyright © 2010 Inderscience Enterprises Ltd.

Reference to this paper should be made as follows: Zupanc, J., Valant, J., Drobne, D., Iglič, V.K. and Iglič, A. (2010) 'A new approach to analyse effects of nanoparticles on lipid vesicles', *Int. J. Biomedical Nanoscience and Nanotechnology*, Vol. 1, No. 1, pp.34–51.

Biographical notes: Jernej Zupanc is a Junior Researcher and a PhD candidate at the Faculty of Computer and Information Science, University of Ljubljana, Slovenia. He is also a Fulbright Scholar and a Visiting Researcher at the Northeastern University, USA. His research interests are in statistical data analysis for the benefit of medical and biological science.

Janez Valant is a Junior Researcher and a PhD candidate at the Biotechnical Faculty, University of Ljubljana. His research interests are focused on nanotoxicology and in vitro toxicity testing of nanoparticles.

Damjana Drobne held the position of Full Professor at the Biotechnical Faculty since 2007 where she is the head of a research group for nanobiology and nanotoxicology. She is a Professor of Zoology and a Professor of Toxiclology. Recently, her research interest is focused toward nanotoxicology. She is studding in vitro and in vivo interactions of nanoparticles and biological systems.

Veronika Kralj Iglič received her BSc, MSc and her PhD from the Department of Physics, University of Ljubljana. Since 2003, she has been an Associate Professor of Biophysics at the University of Ljubljana. At the Faculty of Medicine, University of Ljubljana, she is the Head of Laboratory of Clinical Biophysics. Her interests are biophysics of membranes and biological nanostructures.

Aleš Iglič held the position of Full Professor at the Faculty of Electrical Engineering since 2007, where he is also the Head of Laboratory of Biophysics. His interests are electrostatics and nanobiomechanics of biological membranes.

1 Introduction

Novel properties of engineered nanoparticles offer infinite possibilities in their application, but at the same time they underlie new kinds of biological effects. Nanoparticles differ substantially from bulk materials having the same composition. Properties distinguishing nanoparticles from the bulk material typically become apparent at critical particle lengths below 100 nm. Engineered nanoparticles are recognised as capable of inducing cellular perturbations according to the oxidative stress paradigm and/or by interacting directly with biological membranes (Leroueil et al., 2007). The cell membrane, mitochondria and cell nucleus are considered as major cell compartments relevant for possible nanoparticle-induced toxicity (Unfried et al., 2007).

Recent studies indicate that nanoparticles can strongly interact with cell membranes, either by adsorbing onto the membrane or compromising its integrity (Lipowsky, 1995; Imparato et al., 2005; Linke et al., 2005; Lipowsky et al., 2005; Binder et al., 2007; Liu et al., 2008). When nanoparticles interact with cell membranes, they cause defects such as physical disruptions, formation of holes and thinned regions. Recent papers report *in vivo* and *in vitro* effects of nanoparticles on membrane stability and pore formation (Linke et al., 2005; Hong et al., 2006; Valant et al., 2009). The term hole or pore refers to a wide range of structural changes that could lead to enhanced permeability ranging from the

formation of an actual hole in the membrane to more subtle changes in content of the membrane leading to enhanced diffusion (Antonov et al., 2007). Membrane permeability could arise from a reduction in density of the plasma membrane. In this case, a hole or pore corresponds to a region of reduced material (lipid, protein, cholesterol, etc.). Further, it is well-known that the phase transition of membrane lipids from the liquid crystalline state to the gel is followed by the ion permeability increase (Antonov et al., 1980, 2007). To what extend nanoparticles affect phase transition of membrane lipids and subsequently increase ion permeability is of high importance in all bio-nano interaction studies (Wang et al., 2008a, 2008b).

Size and shape of lipid vesicles are of interest in many scientific studies (Moona et al., 1998; Bagatolli et al., 2000). For example, routine liposome size analysis is carried out by photon correlation spectroscopy (PCS) using commercial instruments. This technique gives a measure for the mean size of the vesicles. Although PCS allows in principle the determination of particle size distributions, the reproducibility and reliability of the method for calculation is insufficient. Quantitative determination of the liposome size distribution, thus, is still difficult. Although a number of powerful approaches like electron microscopy, ultracentrifugation, analytical size exclusion chromatography, and field-flow fractionation have been suggested, none of these approaches has found widespread use due to various limitations.

Until recently, the biophysical behaviour of lipid membranes was not of fundamental importance in toxicological studies. This is rapidly changing with the emergence of nanoparticles and questions regarding their safety. Concerns about cell plasma membrane disruption resulting in toxic effects are also paramount in the minds of nanoparticle designers.

The key issues we are interested in are interactions of nanoparticles with lipid membranes. We hypothesise that manufactured nanoparticles cause defects in lipid vesicles as a result of physical interactions and these effects are demonstrated as shape transformations or a claps of vesicles.

The phospholipid bilayer is the basic constituent of the cell membrane. It is believed that the cell membranes and phospholipid membranes share some important features. Phospholipid vesicles are suitable since the composition of the membrane bilayer can be controlled to some extent. As artificial membranes are much less heterogeneous than cell membranes it is easier to focus on a particular mechanism of interest (Peetla et al. 2009). Also, giant phospholipid vesicles are large enough to be clearly observed live under the phase contrast optical microscope, so some processes such as shape transformations can be directly followed. Vesicles can be made of different lipid compositions while the surrounding solution can be manipulated by adding substances and changing the temperature. It was previously found that some substances can have strong effect on giant phospholipid vesicles, so it would be possible that we would observe such features also due to the presence of nanoparticles (Hungerbuhler et al., 1993; Bensasson et al., 1994,; Zhang and Granick, 2006; Ikeda et al., 2008; Peetla and Labhasetwar, 2009; Peetla et al., 2009).

In the work presented here we studied the effect of fullerene (C_{60}) on artificial phospholipid membranes, which can be readily obtained by forming phospholipid vesicles in water solution. Fullerene are a family of carbon allotropes, molecules composed entirely of carbon, in the form of a hollow sphere, ellipsoid, tube, or plane. Spherical fullerenes are also called buckyballs. Fullerene C_{60} molecules are unique for their multifunctional uses in materials science and optics and are considered for a variety

of biological applications, such as imaging probes, antioxidants and drug carriers (taxol). Data on toxic effects of fullerene were reported already in 2004 (Oberdorster, 2004).

The aim of our work was to study the behavioural changes of populations of lipid vesicles after incubation in a suspension of nanoparticles or a reference chemical by taking advantage of a possibility of direct observation of the vesicles combined with computer aided image analysis approach. The experimental set up is based on analysing and comparing populations of vesicles exposed to nanoparticles or a reference chemical.

2 Materials and methods

2.1 Vesicle preparation

Giant unilamelar phospholipid vesicles were prepared by electroformation from 1-palmitoyl-2-oleoyl-sn-glycero-3phosphatidylcholine (POPC). They were created in saccharose solution and rinsed with equiosmolar glucose solution. Since the intact membrane is impermeable to sugar molecules the sugar composition inside (saccharose) differed from the composition outside (saccharose and glucose). Therefore lipid vesicles appeared darker from the surrounding medium and thus easy for detection. The 45 µl of 5% glucose suspension of was applied on its own object glass. A strip of silicone gel was applied on each side of cover glass to act as a spacer between the cover and the object glass. Subsequently, a droplet of a tested suspension/solution was added to vesicles and finally the other two edges of the cover glass were filled with the silicon past to prevent evaporation.

2.2 Characterisations of nanoparticles

We used transmission electron microscopy and dynamic light scattering (DLS) to characterise C_{60}. Measurements were performed by 3D DLS-SLS spectrometer (LS Instruments, Fribourg, Switzerland). Nanoparticles were dispersed in 100 µg/ml distilled water (see Valant et al., 2009). The mean hydrodynamic radius determined by DLS was 2, 7 and 182 nm. A portion of C_{60} was agglomerated and the size of agglomerates was over the detection limit of the machine (over 1,000 nm). The dispersions of nanoparticles (100 µg/ml) were inspected by DLS using a 3D DLS-SLS spectrometer (LS Instruments, Fribourg, Switzerland). The instrument enables the determination of hydrodynamic radii of particles in extremely turbid suspensions by a so-called 3D cross-correlation technique that successfully eliminates multiple scattering of light. As the light source a HeNe laser operating at a wavelength of 632.8 nm was used. Scattering was measured at an angle of 90°.

2.3 Tested solutions and substances

A solution of $ZnCl_2$ was used as a reference chemical. On the basis of our preliminary studies, concentration 1,000 µg/ml was selected. During the experiment, we added 5 µl of $ZnCl_2$ in 5% glucose to 45 µl of suspension of lipid vesicles (Figure 1). Likewise, the same concentration, 1,000 µg/ml of a suspension of C_{60} was prepared. Here also, 5 µl of C_{60} in 5% glucose was added to 45 µl of suspension of lipid vesicles.

2.4 Experimental setup

In each individual experiment, three object glasses with a suspension of vesicles and tested solution/suspension were inspected. On each object glass, two places: P1 and P2 were chosen where images of vesicles were taken (Figure 1). These places were selected sufficiently apart to allow observing the dynamics of the vesicle behaviour in a concentration gradient. Testing suspension of nanoparticles (C_{60}) and a reference chemical ($ZnCl_2$) were applied close to place P1. Consequently, the concentration of a tested substance at place P1 was higher than at place P2 which is more distant. The aim of this was to create a continuous concentration gradient. The width of each place of imaging is equivalent to the width of field of view of the microscope at the magnification 400×, which is 190 µm. At each place, 15 light microscope images were taken several times during the incubation period. Imaging was performed systematically from the upper toward the lower edge of the object glass. First sets of images were obtained immediately after suspensions of vesicles were applied and covered by cover glasses. In further text these images are referred to as being taken at time zero minutes. The next sets of images were taken after 5 µl of either control (glucose solution), nanoparticles (C_{60}) in a glucose solution or a reference chemical ($ZnCl_2$) in glucose solution were added to vesicles. For the convenience of the analysis, these sets are referred to as being taken after three minutes of incubation. Third and the last sets of images were taken after 90 minutes of incubation.

Figure 1 Sequence of steps in our experiment is presented from left to right (see online version for colours)

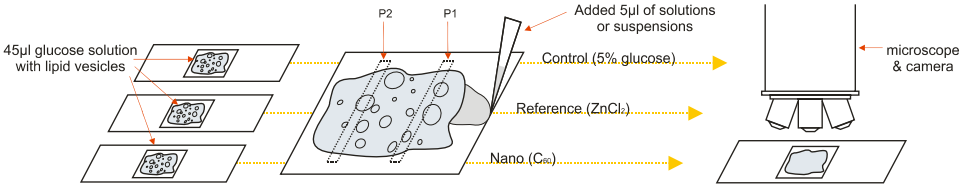

Images were acquired by an invert microscope (Nikon Eclipse TE2000-S) at magnification 400×. This allowed us to capture vesicles with radii larger than 1 µm (largest captured vesicle had a radius of 30 µm). The field of view (visible area) at this magnification is 190 × l43 µm. With 15 images in a vertical session we were able to capture approximately 15% of vesicles at the selected places. Altogether, each experiment with three different solutions was repeated three times.

2.5 Image analysis

As a result of our experiments, a database containing more than 1,600 images was built. All images were labelled so their time, sample group and place on the object glass could be uniquely identified at any later point. Contrast increasing and noise cleaning filters were applied to the images to make the vesicles stand out from the background. The expert used an image editing software to segment all objects of interest [Figures 2(a) and 2(b)]. Because our automatic image segmentation algorithms are not sufficient yet, the expert's segmentation is a very important step of our research. This is the main link

between qualitative and quantitative data, which has to be executed with a high degree of confidence not to spoil our statistical image analysis approach. Furthermore, much information can be added (or lost) at this point and this is why we based this experiment on images labelled by an expert. Attempts that were already made towards automating the image segmentation required for this research are presented in the next chapter.

Next, computer aided image analysis was performed to analyse objects in segmented images. At this point of our research, we were mostly focused on size (presented with vesicle radii, since most of them were circular) and quantity of lipid vesicles in the images. However, other properties and other interesting objects could also be segmented and evaluated in our future work. After the objects were segmented, we were able to link properties of every single vesicle to the solution sample (control, reference or nanoparticles), incubation time (0, 3 or 90 minutes), place on the object glass (P1, P2), and number of the image, where the object was identified.

Figures 2 (a) An example of a light micrograph image (b) image from Figure 2(a) after being labelled

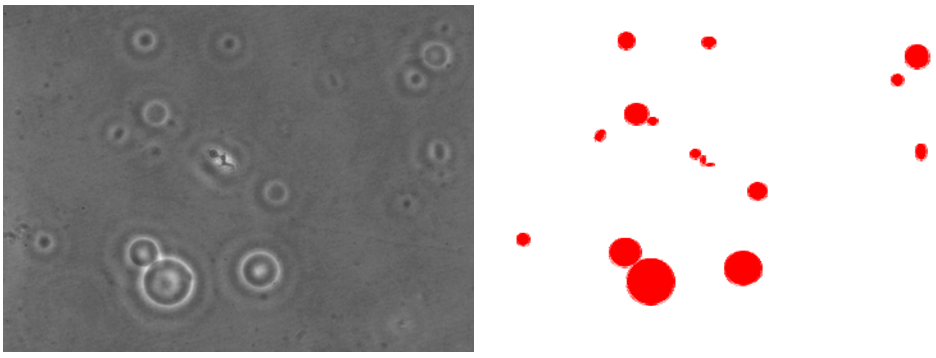

(a) (b)

Notes: Objects (mostly circular) represent segmented lipid vesicles. Their properties are evaluated in our computer aided image analysis.

2.6 Automatic image segmentation

Like in most data mining applications, large amounts of highly informative data are necessary for the connections between different features in our experiment to become obvious and significant. In this respect, the collected images of vesicle population alone are not informative enough. Our long term goal is automatisation the whole image processing in the experiment, but currently the segmentation part has to be done by an expert [Figures 2(a) and 2(b)]. This way, the required information is added by identifying lipid vesicles. From this point on, a completely automated computer aided image analysis was performed to analyse objects in segmented images.

In this experiment, we were mostly focused on size (presented with radii, since most of vesicles were circular) and quantity of lipid vesicles in the images. However, other properties and other interesting objects could also be segmented and will be a task of our future work.

As this is an early stage of our research, automatised image segmentation is not yet satisfactory and cannot replace the manual segmentation by experts. Nevertheless, some

steps in this direction were already made and the results we achieved are promising for our future work towards fully automated image segmentation and feature analysis approach. In this direction, we adapted and tried an algorithm for circle detection - a variation of the adaptive Hough transform, proposed by Illingworth and Kittler (1986), to automatically segment lipid vesicles. Similar algorithm was previously successfully used by Tao et al. to locate positions of individual micro spheres in images obtained by optical section microscopy (Peng et al., 2007). Algorithm takes advantage of the image gradient field, where object boundaries are more determinable compared to intensity field. The image gradient vectors are summed up in an accumulation matrix, where the increased gradients at the edges of circular objects contribute to the accumulation in their centres. A transform is used to convert these gradients into an accumulation matrix. In the latter, intensity of each pixel corresponds to the probability of that pixel being the centre of a circle. Although such centre detection works well for circular lipid vesicles, those with more elliptical eccentricity can still be missed. Our current adaptation of the Hough transform detects approximately 90% of all circles. Since the non-circular lipid vesicles are also a large part of our interest, detecting all elliptical objects (not only circles) is an important goal for our future work.

2.7 Statistical analyses

After more than 20.000 vesicles in 1.600 images were segmented, we analysed their properties. We compared vesicle size distributions of vesicle populations, eccentricities, and quantities. Two-sample Kolmogorov-Smirnov test, for comparing the distributions of values, was used to compare vesicles' size distributions. The null hypothesis is that the (two) compared data vectors with sampled vesicle sizes of vesicle populations are from the same continuous distribution. The alternative hypothesis is that they are from different continuous distributions. The result h is 1 if the test rejects the null hypothesis at the 5% significance level and zero otherwise.

3 Results

3.1 Reproducibility of experimental setup

Reproducibility of the experimental set up was confirmed by running the experiment where only controls, non-treated vesicles, were analysed [Figures 3(a) and 3(b)].

No significant differences were observed in size distribution of control vesicles when different experiments were compared at various durations of exposure. When comparing distributions at the two places [Figures 3(a) and 3(b)], there is a noticeable deviation among distributions at time zero, particularly at place P1. We explain this as a result of initial turbulence in the vesicles solutions immediately after application to the object glass. Interestingly, this deviation is not seen at place P2 at nominal time zero. Here, the size distribution of vesicles is similar to those at three and 90 minutes of observation, as pictures at P2 were taken after those at P1. The turbidity is most probably calmed down already after the initial minutes of placing vesicle solution on the object glass.

Figure 3 Comparison among size distributions of populations of untreated lipid vesicles at places (a) P1 and (b) P2

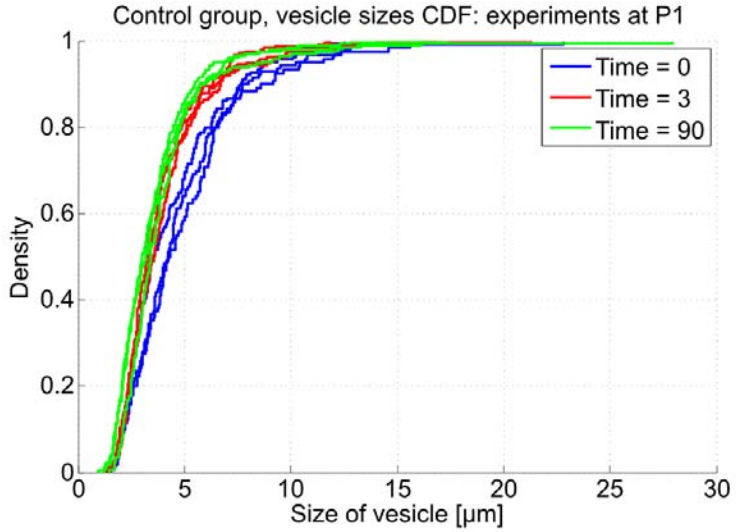

(a)

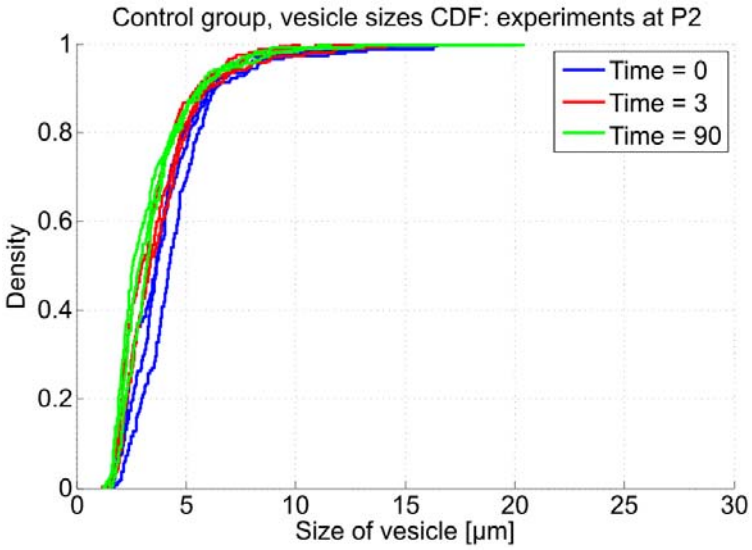

(b)

Notes: Each curve presents cumulative distribution function (CDF) of lipid vesicles' sizes which were observed at a specific time and place on the object glass. Three curves of the same colour represent three experiments while the different colours identify at which time of incubation the properties were measured. These were: the time before adding the tested solution (time = 0), immediately after adding the testing solution (time = 3) and after 90 minutes of incubation (time = 90). In the case of controls, the testing solution was a 5% glucose solution only. The X axis presents sizes of the lipid vesicles in micrometers and F(X) is the cumulative distribution of vesicle size in vesicle populations.

3.2 *Effects of C_{60} and $ZnCl_2$ on lipid vesicles*

Various parameters for describing the behaviour of vesicles in experimental media were observed. These were shape transformations, quantity of vesicles per experimental group and size distribution of a population of vesicles before and after treatment with nanoparticles or a reference chemical.

3.2.1 *Shape transformations of vesicles*

We expected transformations of vesicles from round shaped toward ellipse shaped vesicles. This parameter is described as eccentricity. Since we used Matlab® programming together with image processing toolbox for image analysis the default eccentricity definition it uses can be summarised as:

> "Scalar that specifies the eccentricity of the ellipse that has the same second-moments as the region. The eccentricity is the ratio of the distance between the foci of the ellipse and its major axis length. The value is between 0 and 1. (0 and 1 are degenerate cases; an ellipse whose eccentricity is 0 is actually a circle, while an ellipse whose eccentricity is 1 is a line segment.)"

A comparison of different eccentricities is presented in Figure 4(b). We detected no outstanding differences in the vesicles' eccentricities when different treatments and durations of exposure were compared. In all cases vesicles were predominantly round and deviations from that shape were rare. The average (and median) eccentricity of treated vesicles varied between 0.3 and 0.4 [Figure 4(a)]. No significant and consistent trend toward oval shaped vesicles was observed through time (three or 90 minutes of exposure) or with treatment (controls or C_{60} or $ZnCl_2$ treated vesicles).

Figure 4 (a) Comparison of eccentricities of vesicles after different treatments and different exposure durations, vesicles at places P1 and P2 are presented (b) examples of segmented vesicles with corresponding eccentricity value, 0, 3, 90 – durations of exposure in minutes

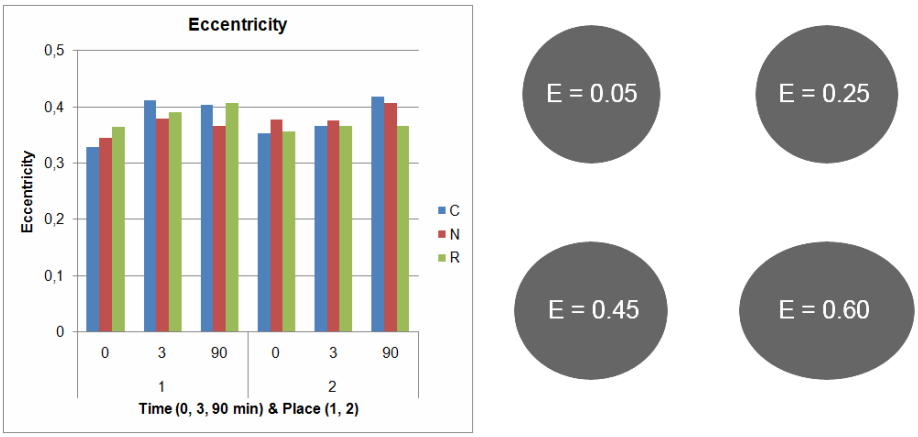

(a) (b)

Notes: C – control, N – nanoparticles, R – reference chemical

3.2.2 Quantity of vesicles

In the experimental set up which we elaborate and present here, quantity of vesicles before and after application of nanoparticles or a reference chemical, was evaluated. In controls, the number of vesicles recorded immediately after addition of a glucose solution was higher as at time 0, which is immediately after application of vesicle solution on the object glass [Figure 5(a)]. During the course of experiment, the number of vesicles in a control group remained constant. Again, we explain this with gravity induced behaviour of vesicles, where vesicles are sedimented after some minutes of being placed on the object glass. The turbidity of a vesicle solution is reduced after first minutes of exposure.

In experiments with the nanoparticles or reference chemical incubated vesicles, significant differences in quantity of vesicles were detected during the course of incubation. At place P1, nanoparticles (C_{60}) or the reference chemical ($ZnCl_2$) significantly reduced the quantity of vesicles [Figure 5(b)]. However, at place P2 only the $ZnCl_2$ solution reduced the quantity of vesicles, while the influence of C_{60} was not noticeable. This could be explained by the fact that the concentration of nanoparticles in the suspension at place P2 is too low to cause collapse of vesicles. Reduction of the concentration of the C_{60} suspension could be due to aggregation of nanoparticles in glucose media or attachment of C_{60} to the vesicles.

Figure 5 Comparison of quantity of lipid vesicles among different treatments and different exposure durations

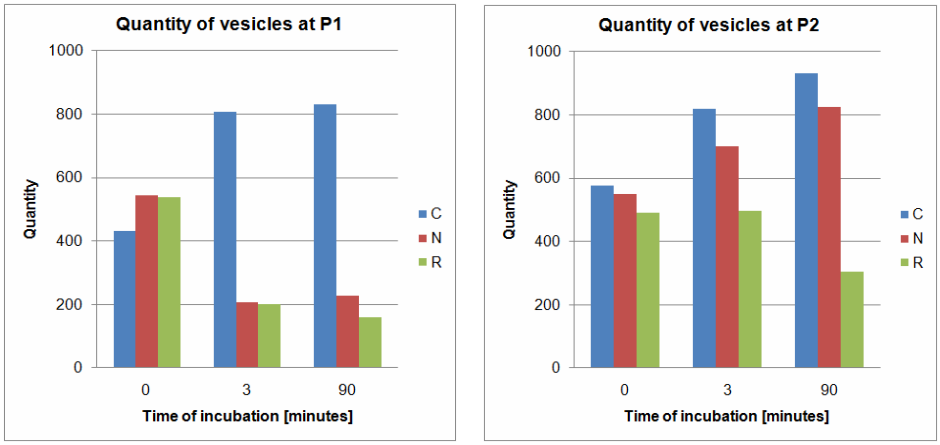

(a) (b)

Notes: Charts respectively present places (a) P1 and (b) P2.
C – control, N – nanoparticles, R – reference chemical.

3.2.3 Size distribution of vesicles

Results in Table 1 show that both nanoparticles and a reference chemical significantly affected the size distribution of vesicles on both tested places (P1 and P2). The difference in size distribution exists also between nanoparticles and $ZnCl_2$.

Figure 6(a) and (b) present cumulative distributions of vesicles' sizes at time zero at both places on the object glass of every inspected group (C, N, R). No noticeable differences can be observed when comparing various curves at this time, because all

suspensions were untreated. However, at nominal time three minutes curves describing size distributions of differently treated vesicles vary evidently. In case of vesicles treated with a reference chemical, the effect can be described as a significant shift toward smaller vesicles. It appears that larger vesicles were affected more drastically resulted in their burst while smaller vesicles remained in less reduced quantities. Interestingly, nanoparticles also affected the vesicles [Figures 5(a) and 5(b)], but size distributions remained similar compared to untreated vesicles.

Table 1 Results of statistical comparison between various vesicle size distribution functions

	Place 1				*Place 2*		
	Experiment	*Result of test*	*Experiment*		*Experiment*	*Result of test*	*Experiment*
Time 0 min	C	1	N	Time 0 min	C	1	N
	C	1	R		C	1	R
	N	0	R		N	0	R
Time 3 min	C	1	N	Time 3 min	C	1	N
	C	1	R		C	1	R
	N	1	R		N	1	R
Time 90 min	C	0	N	Time 90 min	C	1	N
	C	1	R		C	1	R
	N	1	R		N	0	R

Notes: 0 – no significant differences between the groups, 1 – significant differences between the two groups. C – control, N – nanoparticles, R – reference chemical.

Figure 6 Figures a–f describe cumulative distributions of vesicles' sizes at recorded durations of incubation, places and treatments

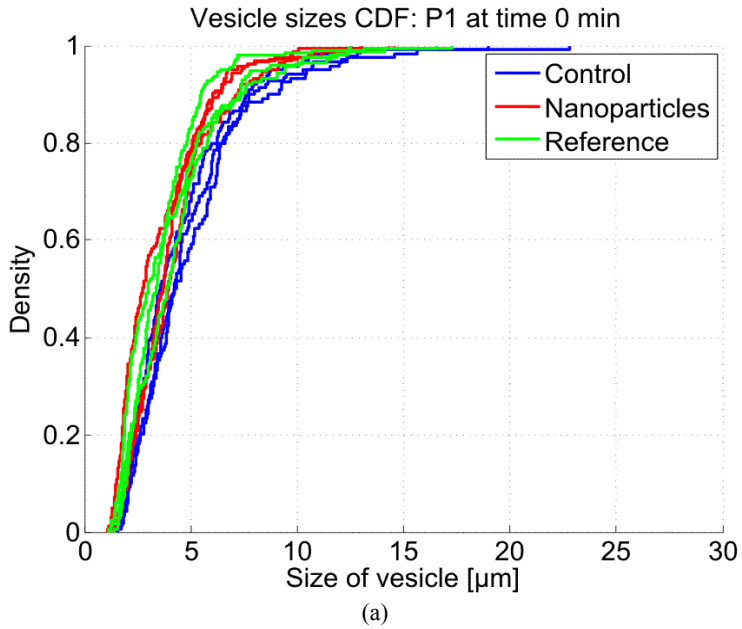

(a)

Notes: Figures a, c and e present distributions of vesicles recorded at place P1 and Figures b, d and f those at place P2 on the object glasses.

Figure 6 Figures a–f describe cumulative distributions of vesicles' sizes at recorded durations of incubation, places and treatments (continued)

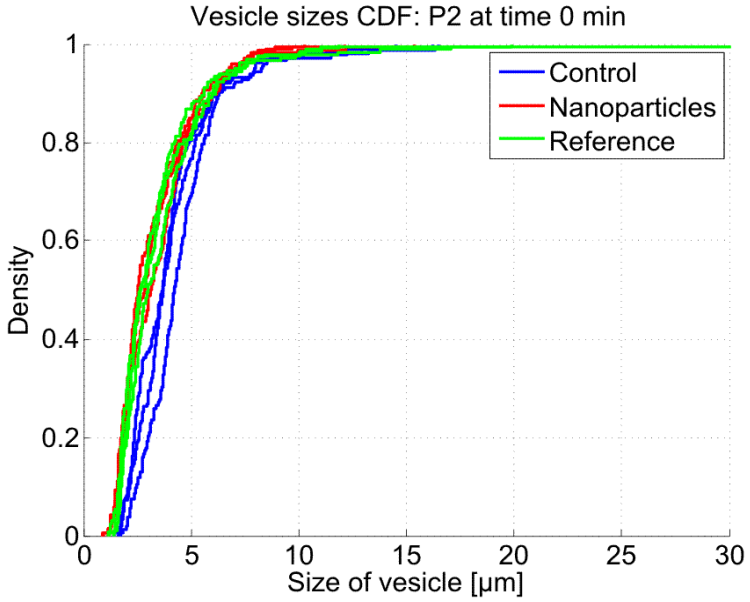

(b)

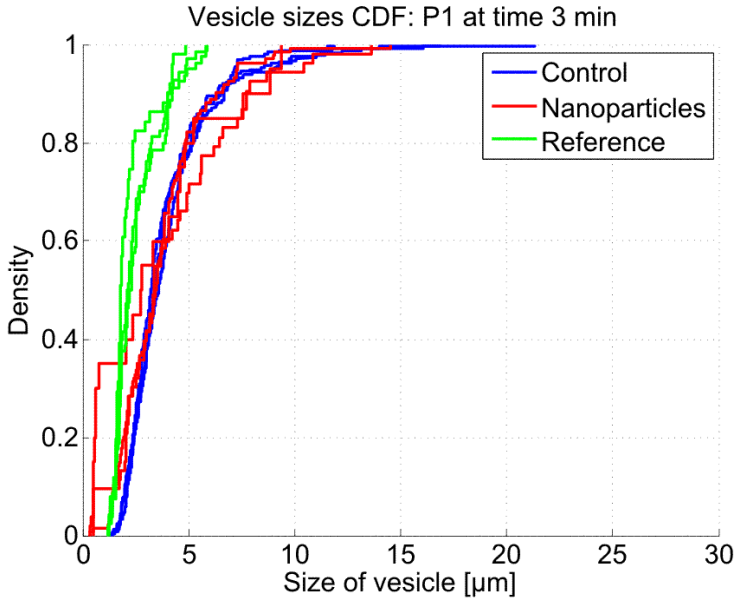

(c)

Notes: Figures a, c and e present distributions of vesicles recorded at place P1 and Figures b, d and f those at place P2 on the object glasses.

Figure 6 Figures a–f describe cumulative distributions of vesicles' sizes at recorded durations of incubation, places and treatments (continued)

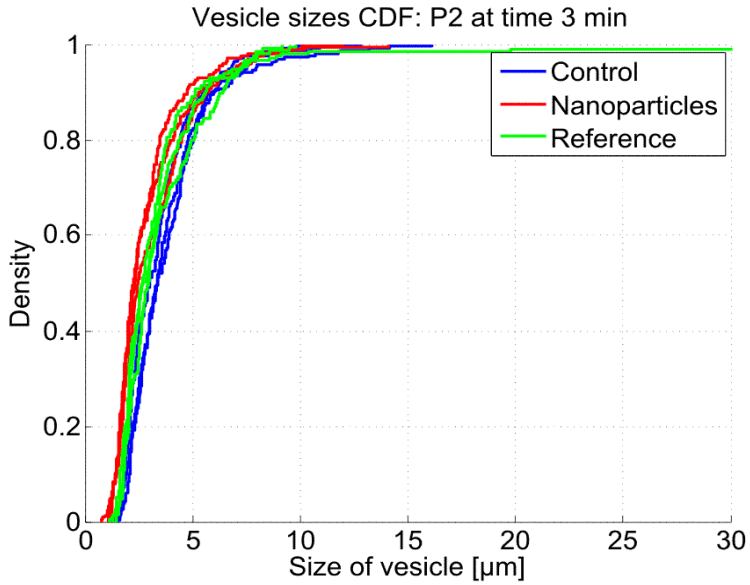

(d)

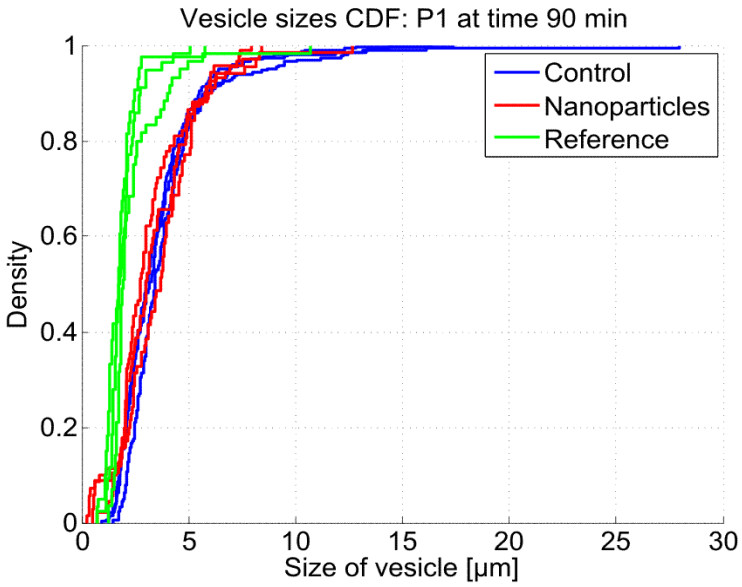

(e)

Notes: Figures a, c and e present distributions of vesicles recorded at place P1 and Figures b, d and f those at place P2 on the object glasses.

Figure 6 Figures a–f describe cumulative distributions of vesicles' sizes at recorded durations of incubation, places and treatments (continued)

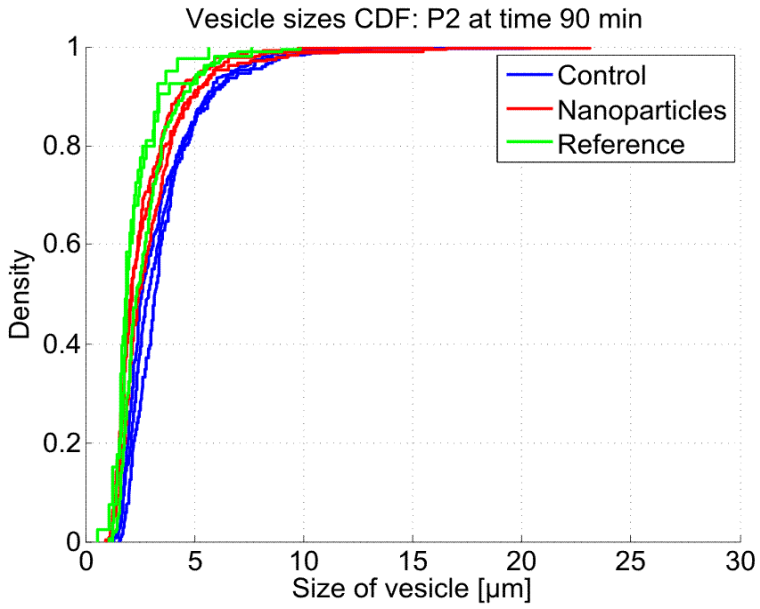

(f)

Notes: Figures a, c and e present distributions of vesicles recorded at place P1 and Figures b, d and f those at place P2 on the object glasses.

By comparing the two places of the same object glass, one can observe that vesicles at place P1 are more affected than those at place P2. We explain this by the concentration gradient, where on place P1 the concentration of the tested substance is higher than on place P2.

4 Discussion

The experimental set up was designed to acquire multiple images of subsets of lipid vesicle populations incubated in different media. Reproducibility and repeatability of the experimental set up was tested by repeated observations and statistical analyses of untreated vesicles. Behaviour of vesicles when interacting with nanoparticles (C_{60}) was described by quantity of vesicles, their shape transformations, and cumulative distribution of vesicles' sizes in vesicle populations.

Many spectroscopy and microscopy methods already exist for describing parameters of lipid vesicle behaviour. However, the method presented here allows recording shape transformations in time and in concentration gradient. This experimental set up is advantageous because it employs statistical image analysis methods and direct microscopy observation of large populations of lipid vesicle.

The results obtained in this study show that tested concentrations of both C_{60} and $ZnCl_2$ have the potential to affect the lipid vesicles. Interactions in our experiments led to a burst of vesicles, which resulted in changed quantities of vesicles and, in the case of $ZnCl_2$, in a significant change in size distribution of vesicles. Shape transformations were not observed to be significantly altered by neither of tested substances. Vesicles' size distribution of a population of vesicles is related to duration of exposure and concentration of tested substance. With the selected parameters we are able to differentiate between effects of the two tested substances (Table 2). Very pronounced differences were detected already after 3 min of exposure to C_{60} or $ZnCl_2$. Data on size distributions of vesicles needs to be interpreted together with data on the quantity of vesicles in order to not underestimate the effect of C_{60} or $ZnCl_2$.

Table 2 Significant differences between treated and untreated populations after three minutes of exposure

	Quantity of vesicles		*Vesicle size distribution of population*	
	Place 1	*Place 2*	*Place 1*	*Place 2*
C_{60}	1	0	1	1
$ZnCl_2$	1	1	1	1

Notes: 1 – statistically significantly different from untreated, 0 – not statistically significantly different from untreated.

Similar data on the potential of C_{60} to interact with biological membranes were reported also by other authors. The damage of C_{60} colloidal suspension to cell membranes was observed both with chemical assays, and confirmed physically by visualising membrane permeability with high molecular weight dyes (Sayes et al., 2005). The results presented by Tang et al., (2008) favour the hypothesis that fullerenes cause more membrane stress than perturbation to energy metabolism.

In is explained that shape transformations of vesicles are governed by curvature and bending elasticity (Lipowsky, 1995; Linke et al., 2005; Imparato et al., 2005). The lipid vesicles could be deflected by osmotic pressure (Mathivet et al., 1996), rising the temperature (Kraus et al., 1995; Ginzburg and Balijepalli, 2007) or electric fields (Kummrow and Helfrich, 1991), or by different surfactants (Babnik et al., 2003). At present stage we cannot explain the mode of action of nanoparticles or $ZnCl_2$ on vesicles. This remains our future task.

$ZnCl_2$ was used in our study as a reference chemical in positive control to provoke the shape transformations of vesicles. In a negative control, vesicles were treated only with glucose solution. Reference chemical appeared to be adequately selected since statistically significant differences between behaviour of control vesicles and those treated with a reference chemical were recorded. Besides, the effects of C_{60} on lipid vesicles were different form that of the reference chemical. This is a proof that the effects are not provoked by experimental conditions (rising temperature, osmotic pressure etc.) but is due to a specific mode of action of the tested substance.

The computer assisted analysis of images obtained by microscopy as presented and discussed here is designed to quantify and validate these perturbations. Further, the potential of this tool to analyse shape transformations of spherical objects in general is considered. Even though our population based approach to identify properties of vesicles proved to be successful, our experimental and computer analysis algorithms still need improvement (Illingworth and Kittler, 2007; Zupanc et al., 2009). In the future, our work

will be focused on adapting and improving methods for automatic vesicle detection (circle and ellipse detection algorithms). Additionally, semi-supervised methods will be studied to combine the knowledge of experts with computer automated approach. When an expert segments a small subset of the images, the information obtained could be used to successfully identify similar objects in other images. Such semi-supervised methods could further improve the percentage of correctly identified vesicles and reduce amount of work required to manually segment images. Consequently, the same amount of expert's work would allow segmentation of even larger lipid vesicles' populations and more relevant and precise calculations.

The lack of methodologies for nanotoxicological evaluation contributes much of the confusion in the current exposure/risk assessment framework, causes uncertainty in the prediction of toxicity of nanoparticulate material and adds to the challenge of bio-nano interaction research (Drobne et al. 2009; Valant et al., 2009). The lack of assessment technology is a critical issue for regulators and investors, agencies who fund the research or industries that expect to profit from the nanotechnology (Borm et al., 2006; Oberdörster et al., 2007). On the basis of present knowledge it appears that lipid vesicles fulfil many requirements to be used in assessment of biological potential of nanoparticles *in vitro*. They are simple models for biological membranes and provide controllable and repeatable experimental conditions. In addition, such *in vitro* systemsare a cost effective mean for toxicological and pharmaceutical studies. A lot of knowledge already exists on interactions between nanoparticles and lipid membranes. This knowledge might significantly contribute to the emerging field of nanotoxicology and support determination of safe doses of nanoparticles for humans and environment.

In the future, studies on lipid vesicles could provide basic understanding of nanoparticle-membrane interactions and more, the information on biological reactivity of nanoparticles could be used as an additional, biological characteristic of nanoparticles apart their physicochemical properties. The method presented here holds many promises for future investigation of the potential of different nanoparticles to interact with lipid membranes. We presented here an approach for studding nanopaticle membrane interactions under highly controlled conditions. The application of machine learning in investigating shape transformations of vesicles illustrates the potential of computational imaging in understanding of the dynamics of nanoparticle-vesicle interactions.

Acknowledgements

We thank D. Erdogmus, D. Skočaj, A. Dobnikar, B. Šter, and U. Lotrič for valuable discussions. We also thank S. Bolte and M. Korošec for their technical assistance.

References

Antonov, V.F., Anosov, A.A., You Nemchenko, O. and Yu. Smirnova, E. (2007) In A. Ottova-Leitmannova, H.T. Tein, (Eds.): *Advances in Planar Lipid Bilayers and Liposomes*, Elsevier, 5. Ed, Amsterdam, pp.151–172.

Antonov, V.F., Petrov, V.V., Molnar, A.A. and Predvoditelev, D.A. (1980) 'The appearance of single-ion channels in unmodified lipid bilayer membranes at the phase transition temperature', *Nature*, Vol. 283, pp.585–586.

Babnik, B., Miklavcic, D., Kanduser, M., Hagerstrand, H., Kralj-Iglic, V. and Iglic, A. (2003) 'Shape transformation and burst of giant POPC unilamellar liposomes modulated by non-ionic detergent C12E8', *Chem. Phys. of Lipids*, Vol. 125, No. 2, pp.123–138.

Bagatolli, L.A., Parasassi, T. and Gratton E. (2000) 'Giant phospholipid vesicles: comparison among the whole lipid sample characteristics using different preparation methods: a two photon fluorescence microscopy study', *Chem. Phys. of Lipids*, Vol. 105, pp.135–147.

Bensasson, R.V., Bienvenue, E., Dellinger, M., Leach, S. and Seta, P. (1994) 'C60 in model biological systems. A visible-UV absorption study of solvent-dependent parameters and solute aggregation', *Journal of Physcal Chemistry*, Vol. 98, No. 13, pp.3492–3500.

Binder, W.H., Sachsenhofer, R., Farnik, D. and Blaas, D. (2007) 'Guiding the location of nanoparticles into vesicular structures: a morphological study', *Phys. Chem. Chem. Phys.*, Vol. 9, pp.6435–6441.

Borm, P.J.A., Robbins, D., Haubold, S., Kuhlbusch, T., Fissan, H., Donaldson, K., Schins, R., Stone, V., Kreyling, W., Lademann, J., Krutmann, J., Warheit, D. and Oberdorster, E. (2006) 'The potential risks of nanomaterials: a review carried out for ECETOC', *Particle Fibre Tox.*, Vol. 3, pp.1–35.

Drobne, D., Jemec, A. and Tkalec, Z.P. (2009) 'In vivo screening to determine hazards of nanoparticles: nanosized TiO2', *Environ. Pollut.*, Vol. 157, No. 4, pp.1157–1164.

Ginzburg, V.V. and Balijepalli, S. (2007) 'Modeling the thermodynamics of the interaction of nanoparticles with cell membranes', *Nano Lett.*, Vol. 7, No. 12, pp.3716–3722.

Hong, S., Leroueil, P.R., Janus, E.K., Peters, J.L., Kober, M.M., Islam, M.T., Orr, B.G., Baker, J.R. and Banaszak Holl, M.M. (2006) 'Interaction of polycationic polymers with supported lipid bilayers and cells: nanoscale hole formation and enhanced membrane permeability', *Bioconjug Chem.*, Vol. 17, No. 3, pp.728–734.

Hungerbühler, H., Guldi, D.M. and Asmus, K-D. (1993) 'Incorporation of C60 into artificial lipid membranes', *Journal of the American Chemical Society*, Vol. 115, No. 8, pp.3386–3387.

Ikeda, A., Sue, T., Akiyama, M., Fujioka, K., Shigematsu, T., Doi, Y., Kikuchi, J., Konishi, T. and Nakajima, R. (2008) 'Preparation of highly photosensitizing liposomes with fullerene-doped lipid bilayer using dispersion-controllable molecular exchange reactions', *Organic Letters*, Vol. 10, No. 18, pp.4077–4080.

Illingworth, J. and Kittler, J. (1986) 'The adaptive Hough transform', *IEEE Trans. Pattern Anal. Mach. Intell.*, pp.690–698.

Imparato, A., Shillcock, J.C. and. Lipowsky, R. (2005) 'Shape fluctuations and elastic properties of two-component bilayer membranes', *Europhys. Letters*, Vol. 69, No. 4, pp.650–656.

Kraus, M., Seifert, U. and Lipowsky, R. (1995) 'Gravity-induced shape transformations of vesicles', *Europhysics Letters*, Vol. 32, No. 5, pp.431–436.

Kummrow, M. and Helfrich, W. (1991) 'Deformation of giant lipid vesicles by electric-fields', *Physical Review*, Vol. 44, No. 12, pp.8356–8360.

Leroueil, P.R., Hong, S., Mecke, A., Baker, Jr, J.R., Orr, B.G. and Banaszak Holl, M.M. (2007) 'Nanoparticle interaction with biological membranes: does nanotechnology present a Janus face? '*Acc. Chem. Res.*, Vol. 40, No. 5, pp.335–342.

Linke, G.T., Lipowsky, R. and Gruhn, T. (2005) 'Free fluid vesicles are not exactly spherical', *Physical Review E*, Vol. 71, No. 5, Article Number: 051602, Part 1.

Lipowsky, R. (1995) 'The morphology of lipid-membranes', *Current Opinion in Structural Biology*, Vol. 5, No. 4, pp.531–540.

Lipowsky, R., Brinkmann, M., Dimova, R., Haluska, C., Kierfeld, J. and Shillcock, J. (2005) 'Wetting, budding, and fusion-morphological transitions of soft surfaces', *Journal of Physics-Condensed Matter*, Special Issue, Vol. 17, No. 31, pp.S2885–S2902.

Liu, J.Z. and Hopfinger, A.J. (2008) 'Identification of possible sources of nanotoxicity from carbon nanotubes inserted into membrane bilayers using membrane interaction quantitative structure-activity relationship analysis', *Chem. Res. Toxicol.*, Vol. 21, No. 2, pp.459–466.

Mathivet, L., Cribier, S. and Devaux, P.F. (1996) 'Shape change and physical properties of giant phospholipid vesicles prepared in the presence of an AC electric field', *Biophysical Journal*, Vol. 70, No. 3, pp.1112–1121.

Moona, M.H., Parka, I. and Kimb, Y. (1998) 'Size characterization of liposomes by flow field-flow fractionation and photon correlation spectroscopy: Effect of ionic strength and pH of carrier solutions', *Journal of Chromatography A*, Vol. 813, No. 1, pp.91–100.

Oberdörster, E. (2004) 'Manufactured nanomaterials (fullerenes, C60) induce oxidative stress in brain of juvenile largemouth bass', *Environ. Health Persp.*, Vol. 112, pp.1058–1062.

Oberdörster, G., Stone, V. and Donaldson, K. (2007) 'Toxicology of nanoparticles: a historical perspective', *Nanotoxicology*, Vol. 1, pp.2–25.

Peetla, C. and Labhasetwar, V. (2009**)** 'Effect of molecular structure of cationic surfactants on biophysical interactions of surfactant-modified nanoparticles with a model membrane and cellular uptake', *Langmuir*, Vol. 25, No. 4, pp.2369–2377.

Peetla, C., Rao, K. and Labhasetwar, V. (2009) 'Relevance of biophysical interactions of nanoparticles with a model membrane in predicting cellular uptake: study with TAT peptide-conjugated nanoparticles', *Mol. Pharmaceut.*, Vol. 6, No. 4, pp.1264–1276.

Peng, T., Balijepalli, A., Gupta, S.K. and LeBrun, T. (2007) 'Algorithms for on-line monitoring of micro spheres in an optical tweezers-based assembly cell', *Journal of Comp. and Inf. Sci. in Eng.*, Vol. 7, No. 4, pp.330–338.

Sayes, C.M., Gobin, A.M., Ausman, K.D., Mendez, J., West, J.L. and Colvin, V.L. (2005) 'Nano-C60 cytotoxicity is due to lipid peroxidation', *Biomaterials*, Vol. 26, No. 36, pp.7587–7595.

Tang, Y.J., Ashcroft, J.M., Chen, D., Min, G., Kim, C-H., Murkhejee, B., Larabell, C., Keasling J.D. and Chen, F.F. (2007) 'Charge-associated effects of fullerene derivatives on microbial structural integrity and central metabolism', Nano letters, Vol. 7, No. 3, pp.754-760.

Unfried, K., Albrecht, C., Klotz, L.O., Von Mikecz, A., Grether-Beck, S. and Schins, R.P.F. (2007) 'Cellular responses to nanoparticles: target structures and mechanisms', *Nanotoxicology*, Vol. 1, pp.52–71.

Valant, J., Drobne, D., Sepčić, K., Jemec, A., Kogej, K. and Kostanjšek, R. (2009) 'Hazardous potential of manufactured nanoparticles identified by *in vivo* assay', *J. Hazard. Material*, Vol. 171, Nos. 1–3, pp.160–165.

Wang, B., Zhang, L., Bae, S.C. and Granick, S. (2008a) 'Nanoparticle-induced surface reconstruction of phospholipid membranes', *PNAS***,** Vol. 105, No. 47, pp.18171–1817.

Wang, L., Nagesha, D., Selvarasah, S., Dokmeci, M. and Carrier, R. (2008b) 'Toxicity of CdSe nanoparticles in Caco-2 cell', *Cultures. J. Nanobiotechnol.*, Vol. 6, No. 1, p.11.

Zhang, L. and Granick, S. (2006) 'How to stabilize phospholipid liposomes (using nanoparticles)', *Nano Lett.*, Vol. 6, No. 4, pp.694–698.

Zupanc, J., Valant, J., Dobnikar, A., Kralj Iglič, V., Iglič, A. and Drobne, D. (2009) 'Interactions of nanoparticles with lipid vesicles: a population based computer aided image analysis approach', *31st Annual International Conference of the IEEE EMBS*, p.T67.